Journal of Applied Physics

Effect of spatial hole burning on output characteristics of high power edge emitting semiconductor lasers: A universal analytical estimate and numerical analysis

Cite as: J. Appl. Phys. **125**, 023108 (2019); https://doi.org/10.1063/1.5055021
Submitted: 05 September 2018 . Accepted: 18 December 2018 . Published Online: 11 January 2019

Eugene A. Avrutin, and Boris S. Ryvkin

Journal of Applied Physics ARTICLE scitation.org/journal/jap

Effect of spatial hole burning on output characteristics of high power edge emitting semiconductor lasers: A universal analytical estimate and numerical analysis

Cite as: J. Appl. Phys. **125**, 023108 (2019); doi: 10.1063/1.5055021
Submitted: 5 September 2018 · Accepted: 18 December 2018 ·
Published Online: 11 January 2019

Eugene A. Avrutin[1,a] and Boris S. Ryvkin[2,3,b]

AFFILIATIONS

[1]Department of Electronic Engineering, University of York, York, United Kingdom
[2]A F Ioffe Physico-Technical Institute, St. Petersburg, Russia
[3]Department of Electrical and Information Engineering, University of Oulu, Oulu, Finland

[a)]Author to whom correspondence should be addressed: eugene.avrutin@york.ac.uk
[b)]Email: ryvkin@switch.ioffe.ru

ABSTRACT

The effect of longitudinal spatial hole burning on the performance of a semiconductor laser with a strongly asymmetric resonator is investigated numerically. The effects of spatial hole burning on, firstly, the non-stimulated recombination in the laser (quantified as an increased effective threshold current) and, secondly, the output efficiency are calculated and compared, and the latter is shown to dominate at high currents. It is shown that the output efficiency at high pumping levels in the presence of the spatial hole burning effect can be estimated using the standard expression as the ratio of output loss to total loss, but with the internal loss enhanced by a factor greater than one and independent on the injection level. A simple universal expression for this factor for a highly asymmetric cavity, as a function of the output mirror reflectance, is obtained and compared to numerical results, with good agreement.

INTRODUCTION

The effect of (*long-range*) longitudinal spatial hole burning (LSHB) in edge emitting semiconductor lasers has been intensely investigated throughout the history of semiconductor laser technology.[1–17] The LSHB effect consists of the inhomogeneous distribution of carrier density, and therefore optical gain, along the laser axis, caused by the inhomogeneous lasing light intensity distribution in the longitudinal direction.[1–10] It is in practice most pronounced in lasers of an asymmetric design, where one mirror is antireflection (AR) coated and the other mirror is high-reflection (HR) coated. Such a design is common in high power lasers. The long range LSHB is thus distinct from *short-range* spatial hole burning, which is due to the standing wave pattern of the laser mode and the associated variation of carrier density on the spatial scale of the laser wavelength, and is more weakly dependent on the mirror reflectances (see, e.g., Ref. 11). Most theoretical approaches to LSHB presented in the literature used either numerical methods of various degrees of complexity[2,7,8] or semi-analytical approaches resulting in complex transcendental formulas that give the spatial dependences of photon and carrier densities in a parametric form.[4,6] Either way, it is not easy to get a generic view of the magnitude of the effect and its dependence on laser parameters, which restricts the conclusions of the analysis to a particular laser construction and operating parameter range. Some analytical progress was made in Refs. 1, 12, and 13. In Ref. 1, an analytical estimate was obtained for the photon density distribution in

almost all the laser cavities (but not for the current dependence of the output power) neglecting non-stimulated recombination. In Ref. 12, we obtained a further simplified estimate for the photon and electron distributions (in the entire cavity) making an additional approximation of negligible intracavity losses. Under those approximations, the carrier distribution was found to stabilize at high currents, and the LSHB was shown to have no direct effect on the laser output (as could be expected from the laws of conservation). The conclusion that *in the absence* of internal losses LSHB has no significant direct effect on the laser performance was confirmed in Ref. 13, where the case of a ring resonator was also treated. It is however well established that *in the presence* of substantial internal absorption, the effect of the LSHB can be a noticeable factor contributing to limiting the output of the laser[8,15] and influencing the laser design,[7,15] particularly if the AR coated mirror has a very low reflectivity (<1%-2% in the construction studied in Ref. 7 and as low as 0.001 in Ref. 15). In Refs. 16 and 17, we attributed the LSHB role mainly to its amplifying the increase in the internal absorption at high injection levels which happens due to other reasons, thus enhancing the *saturation* trend of the laser output (sublinearity of the output curve). The question that has not been answered clearly to date is whether LSHB can be considered a mechanism of this output power saturation in its own right, as well as enhancing other mechanisms of the power curve saturation. This paper seeks to settle this argument definitively, while also shedding more light on LSHB role and nature in general. The analysis concentrates on *direct* effects of LSHB; indirect effects such as any effects of thermal nature contributing to the longitudinal inhomogeneity in the laser are not considered, effectively restricting the treatment to pulsed operating conditions, nor are any lateral effects included in the purely one-dimensional analysis. For more discussions on the limitations of the analysis, see the Discussion and Summary section. While the approximations made by necessity limit the accuracy of the results, they allow for some analytical progress and insight, as discussed in the Analysis section.

ANALYSIS

As in the previous papers (see, e.g., Ref. 12 and references therein), we use for the analytical and numerical study the steady state one-dimensional model consisting of a distributed rate equation for the carrier density N(z) (assuming equal electron and hole densities $N_e = N_h = N$) and the densities of forward and reverse propagating lasing photons $S_f(z)$ and $S_r(z)$

$$\frac{\eta_i i}{eV} - \frac{N}{\tau(N)} - v_g g(S_f + S_r) = 0, \tag{1}$$

$$\frac{dS_f}{dz} = (\Gamma_a g - \alpha_i)S_f, \tag{2}$$

$$\frac{dS_r}{dz} = -(\Gamma_a g - \alpha_i)S_r. \tag{3}$$

Here, i is the pumping current, e the electron charge, η_i the injection efficiency, $V = d_a w L$ the active layer volume (with d_a, w, and L being the active layer thickness, stripe width, and cavity length, respectively), v_g is the group velocity of light in the laser waveguide, g is the carrier density dependent material gain (gain compression due to effects such as spectral hole burning and dynamic carrier heating is much less significant in steady-state analysis than in dynamics). We therefore neglected it in analytical derivations as in Ref. 12, while keeping it for generality in numerical studies as shown below. Furthermore, $\tau(N)$ is the recombination time (other than stimulated recombination), Γ_a is the confinement factor, and, finally, α_i stands for the built-in internal dissipative absorption coefficient in the laser. For the purposes of this model study, α_i is taken as a constant around the length of the resonator and independent on the pumping conditions.

The equations are complemented by the standard reflection boundary conditions at facets at $z = 0, L$, with reflectances R_0 and R_L, respectively,

$$S_r(L) = R_L S_f(L), \tag{4a}$$

$$S_f(0) = R_0 S_r(0). \tag{4b}$$

The output power from the laser is determined as

$$P_{out}(i) = (1 - R_L)v_g w \frac{d_a}{\Gamma_a}\hbar\omega S_f(L), \tag{5}$$

with $\hbar\omega$ being the lasing light quantum.

In the numerical implementation of the model, we ran a time-dependent Travelling Wave model for field amplitudes, with the linewidth enhancement factor set to zero and an artificially narrow gain spectrum to ensure near single-frequency operation, and allowed the simulation to reach steady state. The resulting output power was further time-averaged over 1 ns to smooth out any remaining small traces of satellite longitudinal mode excitation. Such a procedure is equivalent to solving the steady state equations for photon density [(1)–(4)]. For the carrier density dependence of gain, we used a three-parametric logarithmic approximation[18] with gain compression

$$g = g(N, S) = g_0 \ln\frac{N + N_1}{N_{tr} + N_1}\frac{1}{1 + \varepsilon(S_f + S_r)}. \tag{6}$$

Here, the parameters g_0, N_{tr}, and N_1 are the gain constant, the transparency carrier density, and the correction carrier density, respectively, and ε is the gain compression coefficient for numerical simulations. The carrier recombination was assumed to be nearly entirely bimolecular, characterised by the bimolecular recombination coefficient B[18]

$$\frac{1}{\tau(N)} = BN + \frac{1}{\tau_{nr}}, \tag{7}$$

since the analysis was concentrating on lasers operating at wavelengths of around 1μm, where Auger recombination is

TABLE I. The main parameters in the calculations.

Parameter and notation		Value	Units
Bimolecular recombination coefficient	B	1.5×10^{-10}	cm^3/s
Transparency carrier density	N_{tr}	1.8×10^{18}	cm^{-3}
Correction carrier density	N_1	-0.4×10^{18}	cm^{-3}
Gain parameter	g_0	1800	cm^{-1}
Gain compression factor	ε	2×10^{-17}	cm^3
Stripe width	W	100	μm
Active layer thickness	d_a	16	nm
Confinement factor	Γ_a	0.01	
Injection efficiency	η_i	1	

weak and the mature technology makes monomolecular recombination due to material imperfections not too important either (we used $\tau_{nr} = 50$ ns). The parameter values used, unless otherwise indicated in the text, are summarised in Table I.

Typical simulated output curves for a particular laser design ($R_L = 0.01$, $L = 3$ mm) and three values of the internal loss are seen in Fig. 1. For reference, also shown are idealised output curves calculated from the simple lumped rate equation model without the LSHB

$$P_{out}^{(0)}(i) = \frac{\hbar\omega}{e}\eta_i\eta_{out}^{(0)}(i - i_{th});\ \eta_{out}^{(0)} = \frac{\alpha_{out}}{\alpha_{out} + \alpha_i}. \tag{8}$$

In (8), as usual in lumped laser models, $\eta_{out}^{(0)}$ is the output efficiency, and the outcoupling loss is calculated as $\alpha_{out} = \frac{1}{2L}\ln\frac{1}{R_L R_0} \approx \frac{1}{2L}\ln\frac{1}{R_L}$ (we use $R_0 = 0.999 \approx 1$). As could be expected, the reduction of the output power with LSHB taken into account compared to the idealised value $P_{out}^{(0)}$ calculated using (8) is seen to increase with the internal loss value. However, this reduction is not in the form of increasing sublinearity/saturating behavior: the curve $P_{out}(i)$ is to a good accuracy a straight line, albeit with a smaller tangent than the idealised value $P_{out}^{(0)}(i)$.

We proceed next to analyze the nature of the power reduction by LSHB and identify the physical effects at play. Essentially, all the effects of the LSHB stem from the fact that the carrier density (hence recombination current and gain) become progressively inhomogeneously distributed along the cavity length as the current is increased above the threshold. The carrier distributions, normalised to the threshold value, and the photon density/power distribution in the cavity at high currents are shown in Figs. 2(a) and 2(b), respectively, for one representative laser design.

Unlike the case of zero internal losses treated in Ref. 12, we cannot obtain a simple analytical solution for the carrier density profile; on the other hand, the numerical study allows us to calculate the distributions at an arbitrary current, not just at $i \gg i_{th}$ as in Ref. 12. It is seen that at modest currents [$i \sim$ (1-5) i_{th}], there is considerable variation in the carrier density profile with current as the LSHB establishes its effect. For higher currents, the *shape* of the carrier density profile is approximately stabilised (similarly to the analytical results of Ref. 12, where the stabilisation was exact and full). The slow *overall* growth of the carrier density with current is caused by the gain compression, described by the parameter ε and neglected in Ref. 12; it disappears if ε is set to zero.

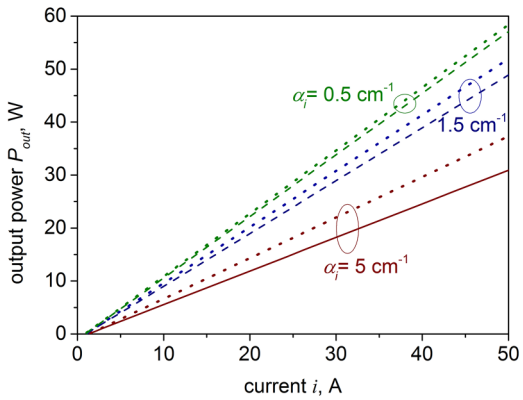

FIG. 1. Output powers in the numerical calculations (bottom curve in each pair) and in the simple lumped model with a constant threshold current $P_{out}^{(0)}$ (top curve) for three values of the internal loss. Wavelength = 0.98 μm.

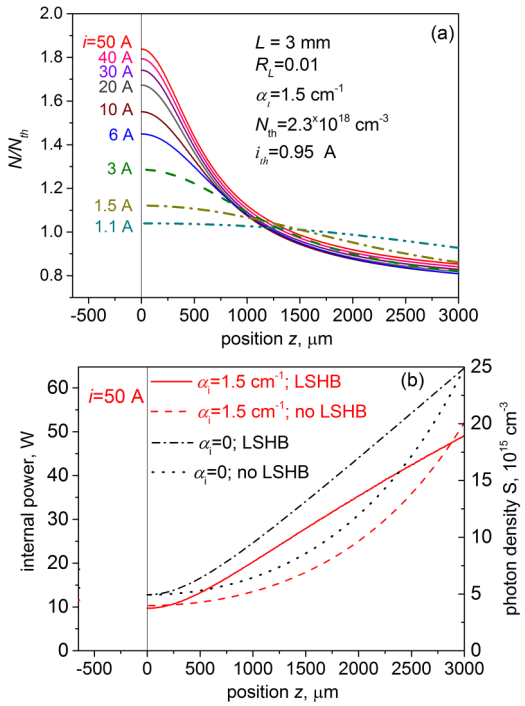

FIG. 2. Effect of LSHB on longitudinal carrier distribution (a) and the internal power distribution (b); the dashed and dotted lines in (b) are the power distribution neglecting LSHB.

As discussed above, it can be analytically shown, and follows from the laws of conservation, that when both non-stimulated recombination and the internal loss can be neglected, the LSHB has no effect on the output power at all. This suggests a heuristic generalisation of (8) for the output power with LSHB as[16,17]

$$P_{out}(i) \approx \frac{\hbar\omega}{e}\eta_i\eta_{out}(i)[i - i_{th}^{eff}(i)]. \quad (9)$$

The two distinctions between (9) and the simple "lumped" formula (8) represent the two mechanisms via which LSHB directly affects the laser output. The first mechanism, present even in the absence of internal losses and already briefly discussed in our previous paper,[12] is to do with the fact that the strongly inhomogeneous carrier distribution in the laser along the cavity length under LSHB conditions [Fig. 2(a)] makes the current spent on non-stimulated recombination [the effective threshold current $i_{th}^{eff}(i)$ at a pumping current i] greater than the actual threshold current i_{th} and, in general, dependent on the pumping level i. The current is evaluated as[12]

$$i_{th}^{eff}(i) = \frac{ewd_a}{\eta_i}\int_0^L \frac{N(z,i)}{\tau[N(z,i)]}dz. \quad (10)$$

As discussed in Ref. 12, the threshold modification by LSHB is absent, and thus $i_{th}^{eff}(i) \equiv i_{th}$, if the gain-carrier density dependences of the gain and (non-stimulated) recombination rate are both linear; however, in realistic Quantum Well materials typically used in high-power lasers, and hence in our simulations, the former dependence is sublinear (logarithmic) and the latter superlinear (quadratic), meaning that $i_{th}^{eff}(i) > i_{th}$ for $i > i_{th}$.

The second mechanism takes into account the fact that the LSHB affects the output efficiency $\eta_{out}(i)$ of the laser. Equation (9) is, formally, the definition of this parameter, assuming P_{out} is calculated from a distributed model, and the effective threshold, from Eq. (10). Physically, as in a lumped model, $\eta_{out}(i)$ represents the relation between, on the one hand, the average photon density inside the laser and, on the other hand, the output power, proportional to the density of outbound photons at the output facet.

The nature of the output efficiency modification by LSHB can be seen most clearly for small to moderate internal losses, such as the case shown in Fig. 2(b). Indeed, let us compare the longitudinal distribution of the photon density S, or the internal power $P(z) = v_g\hbar\omega\frac{wd_a}{\Gamma_a}S(z)$, along the cavity with LSHB taken into account [straight line in Fig. 2(b)] to the S(z) distribution calculated with LSHB neglected [with $N(z) \approx N_{th}$ used instead of the electron density distribution of Fig. 2(a); dashed line in Fig. 2(b)]. It is seen in the figure that, while the output power, and thus $P(z \approx L)$, is slightly lower in the presence of LSHB than in the $N(z) \approx N_{th}$ case (the difference is relatively small though so long as α_i is small, and completely absent if $\alpha_i = 0$, also shown in the figure for reference), the value of S(z) in the *bulk* of the laser is noticeably higher in the presence of LSHB than in its absence. Thus, the average photon density $\overline{S} = \frac{1}{L}\int_0^L S(z)dz$ and the total number of photons absorbed in the cavity per unit time $v_g\alpha_i\frac{wd_aL}{\Gamma_a}\overline{S}$ are increased in the presence of LSHB compared to the approximation of a longitudinally constant N (no LSHB). With this picture in mind, it is convenient to describe the reduction of η_{out} by LSHB in the heuristic form

$$\eta_{out}(i) = \frac{\alpha_{out}}{f_{LSHB}(i)\alpha_i + \alpha_{out}} = \frac{\alpha_{out}f_{LSHB}^{-1}(i)}{\alpha_i + \alpha_{out}f_{LSHB}^{-1}(i)}. \quad (11)$$

The dimensionless "LSHB factor" $f_{LSHB}(i) > 1$ can thus be interpreted either as an effective *enhancement* of the internal loss in the laser cavity[16,17] (seeing that at a given current, more photons per unit time are absorbed in the cavity with LSHB taken into account than neglecting it) or, alternatively, as effective *reduction* in the output losses (since in a calculation taking into account LSHB, a smaller fraction of the average internal photon density, or total photon number, leaves the cavity than when LSHB is neglected). The value of $f_{LSHB}(i)$ depends on current and also on the parameters of the laser structure and will be discussed in more detail below.

The variation of carrier density profile with the current described above (significant variation at low currents with subsequent stabilisation at higher currents) determines the current dependence of both the effective threshold current $i_{th}^{eff}(i)$ and the factor $f_{LSHB}(i)$. We first quantify the first effect, the increase in the effective threshold with the current. This is shown in Fig. 3, with the effective threshold current evaluated using (10).

As can be expected given the carrier density variation in Fig. 2, the effective threshold current [which at threshold equals the actual threshold current: $i_{th}^{eff}(i_{th}) = i_{th}$] increases fast with i at small excess currents above the threshold. At high

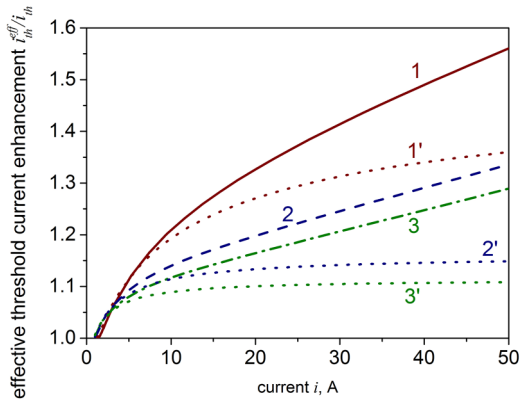

FIG. 3. Effective threshold current increase over the actual threshold current, as a function of current for the laser parameters as in Figs. 1 and 2. 1,1′—$\alpha_t = 5\ cm^{-1}$; 2,2′—$\alpha_t = 1.5\ cm^{-1}$; 3,3′—$\alpha_t = 0.5\ cm^{-1}$; 1,2,3—ε as in Table I; 1′,2′,3′—$\varepsilon = 0$.

currents, it increases with the current much slower, and in an approximately linear fashion, due to the gain compression (note that in the dotted curves 1′,2′,3′, calculated with $\varepsilon = 0$, this slow linear increase is absent and the effective threshold settles at a constant value). We can then calculate what correction the threshold modification, as well the LSHB effects as a whole, make to the laser output by calculating the total relative power correction

$$\delta P_{total}^{LSHB}(i) = \frac{P_{out}^{(0)}(i) - P_{out}(i)}{P_{out}^{(0)}(i)}, \tag{12}$$

and the relative power correction $\delta P_{th}^{LSHB}(i)$ due to the threshold increase only. The latter is calculated as $\delta P_{th}^{LSHB}(i) = \frac{P_{out}^{(0)}(i) - P_{out}^{(th)}(i)}{P_{out}^{(0)}(i)}$, where $P_{out}^{(th)}(i) = \frac{\hbar\omega}{e}\eta_i\eta_{out}^{(0)}[i - i_{th}^{eff}(i)]$ is the power that would be emitted by the laser if the effective threshold modification were the only effect of LSHB. From this, using (8), we obtain

$$\delta P_{th}^{LSHB}(i) = \frac{i_{th}^{eff}(i) - i_{th}}{i - i_{th}}. \tag{13}$$

Both of these relative corrections are shown in Fig. 4 as functions of current. From this figure (which corresponds to two of the light-current curves of Fig. 1), it is seen that at low power (close to threshold), the effect of the LSHB is to a substantial extent determined by the effective threshold current increase. At high currents, as the denominator of (13) increases, the relative effect of the threshold enhancement on the current decreases, with $\delta P_{th}^{LSHB}(i)$ settling to a small constant value (in the absence of gain compression, it would tend to zero).

The *total* relative LSHB-induced correction to power $\delta P_{total}^{LSHB}(i)$ increases with the current at small to moderate injection levels, as the slope of the curve decreases from what is essentially the lumped-model value at the threshold to the lower value seen at high injection levels. At high currents, the value of $\delta P_{total}^{LSHB}(i)$ stabilises at a constant value which substantially exceeds the correction $\delta P_{th}^{LSHB}(i)$ due to modification of effective threshold and is dominated by the second of the LSHB effects, the modification of the output efficiency $\eta_{out}(i)$. This is consistent with the known fact that under high current operation, when $i \gg i_{th}$, it is the differential quantum efficiency of the laser, rather than the threshold, that has the most important effect on the $P_{out}(i)$ curve.

We proceed then to calculate the LSHB factor, characterising the decrease in $\eta_{out}(i)$, as a function of current from the numerically simulated curves, by resolving the expressions (9) and (11) for $f_{LSHB}(i)$

$$f_{LSHB}(i) \approx \frac{\alpha_{out}}{\alpha_{in}}\left\{\frac{\hbar\omega}{eP_{out}(i)}\eta_i\left[i - i_{th}^{eff}(i)\right] - 1\right\}. \tag{14}$$

The results of this procedure are shown in Fig. 5 for several values of internal loss and reflectance coefficients. It is seen that, as can be expected from Fig. 4, at moderate currents, the value of $f_{LSHB}(i)$ increases monotonically with the current, whereas at high currents, it appears to reach a constant limit $f_{LSHB}^{lim} = \lim_{i\to\infty} f_{LSHB}(i) > 1$. The value of f_{LSHB}^{lim} decreases with the output facet reflectance coefficient R_L and increases somewhat with the internal loss coefficient.

In order to confirm that f_{LSHB}^{lim} is indeed a limit value in the mathematical sense, an analytical solution of the system (1–4) is required. As mentioned in the Introduction, only limited analytical progress leading to transcendental equations[6] is possible in the generic case of an arbitrary internal loss. However, we note that, while the assumption of zero

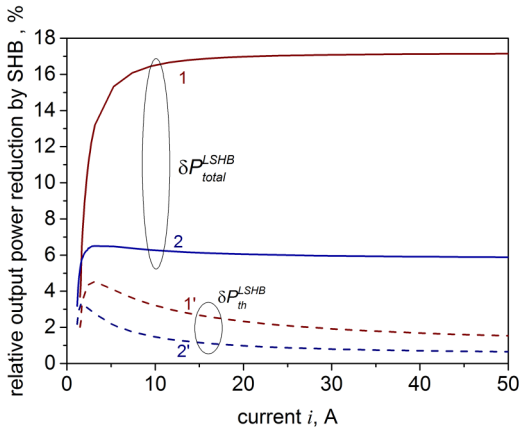

FIG. 4. Reduction in the output power due to the effective threshold current increase (1′,2′) and the total power reduction by LSHB (1,2), normalised to the power in the lumped model, for a laser with $L = 2$ mm, $R_L = 0.01$, and the internal loss $\alpha_i = 5$ cm^{-1} (1,1′) and 1.5 cm^{-1} (2,2′).

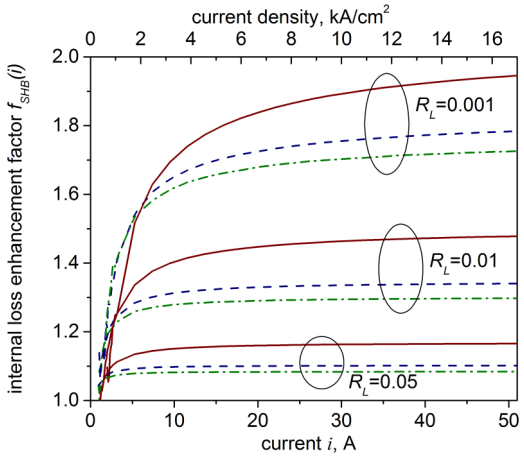

FIG. 5. The LSHB factor (extracted from numerical simulations) as a function of current for three values of the output facet reflectance and for the internal loss of 5 cm^{-1} (solid), 1.5 cm^{-1} (dashed), and 0.5 cm^{-1} (dash-dotted).

loss $\alpha_{in} = 0$ made in Ref. 12 is in practice unattainable, all practical lasers are designed to have a small to moderate built-in loss $\alpha_{in}L \ll 1$. Making the small loss assumption (to be quantified below), assuming in addition negligible non-stimulated recombination, and setting $\varepsilon = 0$ and $R_0 = 1$ as mentioned above, it is possible (see the Appendix for the derivation) to confirm that the LSHB factor does indeed tend to a constant value f_{LSHB}^{lim} in the high injection limit. The procedure allows us to obtain a simple and universal analytical estimate for f_{LSHB}^{lim} which turns out to be a function of *only one parameter*, the output facet reflectance, in the form of

$$f_{LSHB}^{lim} \approx \frac{1}{4}\left[\frac{1+R_L}{1-R_L} + \frac{2R_L}{(1-R_L)^2}\ln\frac{1}{R_L}\right]\ln\frac{1}{R_L}. \quad (15)$$

This expression is one of the central results of this paper. The fact that the coefficient f_{LSHB}^{lim} is independent of power/current proves that the spatial hole burning in itself, as suggested in Ref. 12, is not a distinct mechanism behind the saturating trend of the light-current curve (sublinear dependence of power on current) at high currents/powers, even in the presence of internal losses. Rather, it just modifies the output efficiency to a value of $\eta_{out}^{LSHB} = \frac{\alpha_{out}}{\alpha_{out}+f_{LSHB}^{lim}\alpha_i}$ that is smaller than the small-signal value $\eta_{out}^{(0)}$ as defined by Eq. (8), but does not depend on the current or power other than through the internal loss α_i. Thus, if the internal loss can be considered constant, the laser output efficiency will stay constant as well and so will the total efficiency once the condition $i \gg i_{th}^{eff}(i)$ is satisfied (which is known to be the case at relatively modest currents).

The fact that f_{LSHB}^{lim} only depends on R_L means that the high-current output efficiency $\eta_{out}^{LSHB} = \frac{\alpha_{out}}{\alpha_{out}+f_{LSHB}^{lim}\alpha_i}$, and thus the effect of the LSHB on the output of the laser, can be roughly estimated using the expressions (9)–(11) and (15) from the values of α_i and R_L, without the need to solve the spatially distributed system [(1)–(4)] numerically. Clearly, the estimate will be the more accurate, the smaller the value of the internal losses [since expression (15) was derived in the assumption of weak internal absorption]. Figure 6 shows the numerically calculated values of f_{LSHB}^{lim} for different cavity lengths, output facet reflectances, and internal loss values. It is seen that for small internal absorption ($\alpha_i = 0.5\,cm^{-1}$), the agreement between the numerical results and the analytical formula (15) is excellent, and for the intermediate absorption value ($\alpha_i = 1.5\,cm^{-1}$, or $\alpha_i L \sim 0.3 - 0.9$ for the cavity lengths shown), it stays good—indeed, the applicability limit of Eq. (15) is $\alpha_i L \ll \frac{1}{\sqrt{R_L}}$ rather than $\alpha_i L \ll 1$ (see the Appendix), so the formula can still work reasonably well for values of $\alpha_i L \sim 1$. Even at $\alpha_i = 5\,cm^{-1}$

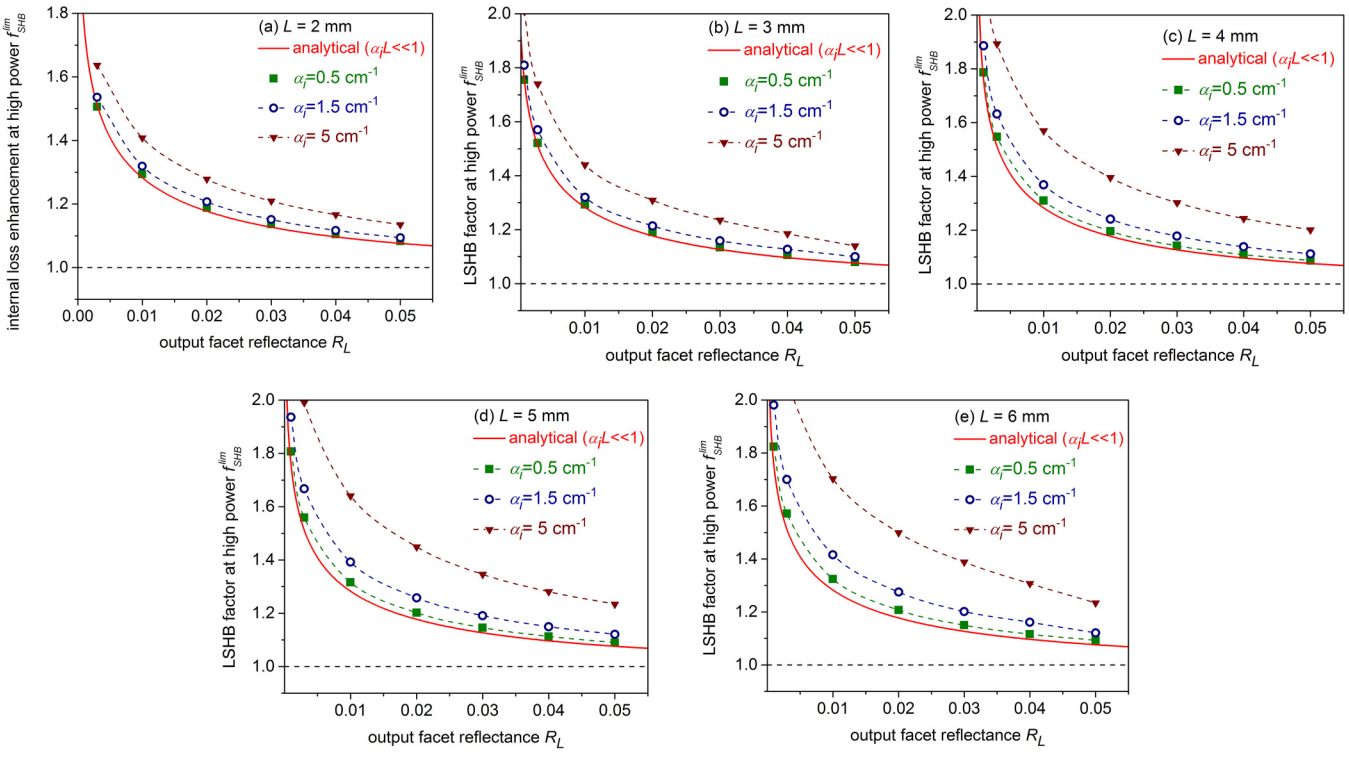

FIG. 6. High-power limit of the LSHB factor as a function of the output facet reflectance: analytical (solid line) and numerical (points).

(which, strictly speaking, no more satisfies *any* condition of weak absorption, particularly for long cavities), there is a *reasonable* agreement between the simulations and the analytical theory, and the correct tendency is reproduced in numerical results—the factor f_{LSHB}^{lim} decreases with R_L, tending to one when R_L approaches one (in which case, there is no LSHB). For a more accurate estimate, the value of f_{LSHB}^{lim} can be taken directly from the numerical points in Fig. 6 (hence we are showing these results here for a number of parameter values for reference purposes).

We note that, as in previous studies, any appreciable effect of LSHB is only seen for $R_L < \sim 0.01$, and in most cases the value of f_{LSHB}^{lim} is no greater than approximately 2–2.5 in all cases considered (Fig. 6). Thus, the LSHB effect, even at output reflectances as small as ~0.01, becomes important only for values of internal absorption that are relatively substantial, particularly by the standards of modern technology ($\alpha_i L \sim 1$).

DISCUSSION AND SUMMARY

It has to be noted that, while the agreement between analytical and numerical results shown in Fig. 6 proves that the analytical result (15) is an accurate enough approximate solution to the system of Eqs. (1)–(4), it leaves open the issue of how accurately system [(1)–(4)] itself describes a practical high-power laser, or in other words of the possible importance of physical effects not included in the model. Indeed, to begin with, the analysis here, in common with a number of studies in the literature (see, e.g., Refs. 7, 8, 16, 17, and 19), is one-dimensional, leaving aside the laterally multimode nature of the broad-area laser emission. Such an approach is most rigorously justified for a narrow-stripe single lateral mode laser (the results for such a design can be obtained by scaling the stripe width, the current, and the power in our calculations down by the same factor of 30–50). When applied to a broad-area laser with parameters as in Table I, the model effectively assumes that there are so many lateral modes in the laser emission that the light intensity, averaged over time, fills the entire stripe approximately evenly. We also ignore the interplay of longitudinal and lateral nonuniformity in self-heating,[19] effectively restricting the analysis to a pulsed operating regime.

Our analysis also relies on the internal loss coefficient's being constant along the length of the laser. Estimate (15) is thus not straightforwardly applicable to the internal loss caused directly and/or indirectly by two-photon absorption (TPA; see Ref. 20 and references therein) which is by its nature very inhomogeneous along the laser cavity, although a longitudinally averaged value can possibly be used at least in the first approximation. Likewise, the relation between the active layer carrier density (which also varies along the laser length due to LSHB) and the internal absorption was ignored—we deliberately took the internal absorption coefficient as a pre-defined constant to quantify its effect on LSHB explicitly. We note finally that the analysis here, both numerical and analytical, only dealt with *direct* effects of the LSHB. As mentioned in previous studies,[12] LSHB will affect the efficiency more significantly in the case of the carrier density at the HR coated facet becoming so high as to contribute to the carrier leakage from the active layer to the Optical Confinement Layer (OCL), which is particularly important at increased temperatures.[21] This *indirect* effect (which, like the effects of TPA, is inhomogeneous along the cavity length) may have been one of the causes of the additional saturation tendency of the $P_{out}(i)$ curve seen in some numerical studies[8,14] when LSHB was included in the calculations, particularly as the authors used a fairly small R_L value ($R_L = 0.01$ was used in Refs. 8 and 14).

The additional effects discussed above need to be taken into account for detailed, inclusive modeling of a practical laser design. The purpose of the current paper was to isolate, as much as possible, the primary, direct effects of LSHB and their physical nature. The results can be summarized as follows:

We have shown that at low currents, the dominant direct effect of the LSHB was the increase in the non-stimulated recombination (effective threshold) current, whereas at high currents, the modification of output efficiency (which can be seen as an effective enhancement of the internal losses or equivalent effective reduction of output losses) dominated. We found the factor characterizing this effective loss enhancement by LSHB at high currents to stabilize at a constant value f_{LSHB}^{lim} and found a simple analytical estimate for this value, for the case of low to moderate internal losses and a strongly asymmetric cavity (non-output facet reflector ≈ 1), as a function of only the output facet reflectance. A good agreement was found between this analytical estimate and numerical simulations, provided that the internal losses remained substantially smaller than the outcoupling losses. We believe the results prove definitively that in the high current limit, the LSHB is *not* a distinct mechanism behind the saturating trend (sublinear behavior) of the power vs current curve, but just increases the effect of other power saturation mechanisms, primarily the increase in internal losses with the power/injection level. If optical losses at high power can be evaluated, our analysis allows the effect of LSHB on the output efficiency to be estimated without solving the spatially resolved model, using the analytical expression (15) as a first-order estimate or numerically calculated f_{LSHB}^{lim} (Fig. 6) for better accuracy. While the numerical calculations were performed for a representative Quantum Well near-infrared laser, the analytical expression (15) applies for any class B laser including, for example, Quantum Cascade lasers analyzed in Ref. 13.

APPENDIX: THE DERIVATION OF THE HIGH-CURRENT VALUE OF THE LSHB FACTOR

For obtaining an analytical estimate of the output power, we return to the system of Eqs. (1)–(4) and follow previous work (see, e.g., Refs. 2, 5, 6, and 12) in noting that the nature of Eqs. (2) and (3) means that the product $S_f(z)S_r(z) = \text{const}(z) = S_0^2$. One of the two differential equations, say (3), is then eliminated, and the constant S_0 is determined when solving the system (1) and (2) with boundary conditions (4). In order to do

so, as in previous work, we restrict the analysis to the case of high injection levels when all non-stimulated recombination can be neglected. Then, the gain can be expressed formally from (1) as a function of photon density, and the problem is reduced to a single equation for S_f[6]

$$\frac{dS_f(z)}{dz} = \frac{a}{L}\frac{S_f^2(z)}{S_f^2(z)+S_0^2} - \alpha_i S_f(z), \tag{A1}$$

with $a = \frac{\Gamma_a \eta_i i}{v_g e w d_a}$. Setting $R_0 \approx 1$, a simple estimate for S_0 for the case of $\alpha_{int} = 0$ is obtained[12]

$$S_0 = a s_0;\ s_0 = \frac{\sqrt{R_L}}{1-R_L}. \tag{A2}$$

In the general case, separating variables in (A1) and introducing normalized variables

$$s = \frac{S_f}{S_0};\ x = \frac{a}{S_0}\frac{z}{L};\ b = \frac{S_0}{a}\alpha_i L,$$

results in a normalized form of (A1): $\frac{ds}{dx} = \frac{s^2(x)}{s^2(x)+1} - bs(x)$, which after separation of variables has a formal solution

$$\int_1^s \frac{dt(t^2+1)}{t[t-b(t^2+1)]} = x.$$

In general, this results in transcendental equations as in Ref. 6; however, in the case of $b \ll 1$, a first order Taylor expansion in b gives

$$\int_1^s \frac{dt(t^2+1)}{t^2}\left[1+\frac{b}{t}(t^2+1)\right] = x,$$

so

$$s - \frac{1}{s} + b\left(\frac{s^2}{2} + 2\ln s - \frac{1}{2s^2}\right) = x. \tag{A3}$$

At the output facet ($z = L$), we have $x = \frac{a}{S_0}$ and from the reflectance condition (4a), $s = \frac{1}{\sqrt{R_L}}$.

Substituting these values into (A3) gives a correction to the value of s_0, and hence to the output power, in the first order in the small parameter b. Using the value of s_0 at $\alpha_{int} = 0$ to approximate $b = \frac{\sqrt{R_L}}{1-R_L}\alpha_i L$ and returning to dimensional units, we obtain an estimate for S_f at the output facet in the form of

$$S_f(L) \approx \frac{a}{1-R_L}\left[1 + \frac{\alpha_i L}{2}\frac{R_L}{(1-R_L)^2}\left(\frac{1-R_L^2}{R_L} + 2\ln\frac{1}{R_L}\right)\right]^{-1}.$$

Comparing this to the value without LSHB

$$S_f^{no\ LSHB}(L) = \frac{a}{1-R_L}\frac{\alpha_{out}}{\alpha_{out}+\alpha_i} = \frac{a}{1-R_L}\left[1 + 2\alpha_i L\left(\ln\frac{1}{R_L}\right)^{-1}\right]^{-1},$$

we obtain the estimate [Eq. (15)]

$$f_{LSHB}^{lim} \approx \frac{1}{4}\left[\frac{1+R_L}{1-R_L} + \frac{2R_L}{(1-R_L)^2}\ln\frac{1}{R_L}\right]\ln\frac{1}{R_L}.$$

The limit of its validity is estimated as $b \ll 1$, so $\alpha_i L \ll \frac{1-R_L}{\sqrt{R_L}}$ which is somewhat more relaxed (since $R_L \ll 1$) than $\alpha_i L \ll 1$.

REFERENCES

[1]W. W. Rigrod, "Saturation effects in high-gain lasers," J. Appl. Phys. **36**, 2487 (1965).
[2]C. H. Gooch, "A theory of the high-power operation of gallium arsenide lasers," in *Proceedings of the International Symposium on* GAAs (Institute of Physics, 1966), pp. 62–67.
[3]Y. Nannichi, J. Appl. Phys. **37**, 3009 (1966).
[4]W.-C. W. Fang, C. G. Bethea, Y. K. Chen, and S. L. Chuang, IEEE J. Select. Top. Quantum Electron. **1**, 117 (1995).
[5]A. J. Bennett, R. D. Clayton, and J. M. Xu, J. Appl. Phys. **83**, 3784 (1998).
[6]A. J. Bennett, E. H. Sargent, R. D. Clayton, H. B. Kim, and J. M. Xu, Proc. SPIE **3004**, 160 (1998).
[7]F. Rinner, J. Rogg, P. Friedman, M. Mikulla, G. Weimann, and R. Poprawe, Appl. Phys. Lett. **80**, 19 (2002).
[8]H. Wenzel, P. Crump, A. Pietrzak, X. Wang, G. Erbert, and G. Tränkle, New J. Phys. **12**, 085007 (2010).
[9]R. Ulbrich and M. H. Pilkuhn, Appl. Phys. Lett. **16**, 516 (1970).
[10]R. Ulbrich and M. H. Pilkuhn, IEEE J. Quantum Electron. **6**, 314 (1970).
[11]C. B. Su, Electron. Lett. **24**, 370 (1988).
[12]B. S. Ryvkin and E. A. Avrutin, J. Appl. Phys. **109**, 043101 (2011).
[13]T. Mansuripur, G.-M. De Naurois, A. Belyanin, and F. Capasso, Optica **2**, 48 (2015).
[14]J. Piprek and Z.-M. Li, Photon. Technol. Lett. **30**, 963 (2018).
[15]H. Wenzel, IEEE J. Select. Top. Quantum Electron. **19**, 1502913 (2013).
[16]E. A. Avrutin and B. S. Ryvkin, "Theory and modelling of the power conversion efficiency of high power large optical cavity laser diodes," in *Proceedings of the 2nd International Conference on High Power Diode Lasers and Systems*, Coventry, UK, 14–15 Oct 2015 (IEEE, 2015), pp. 9–10.
[17]E. A. Avrutin and B. S. Ryvkin "The role of carrier accumulation in the optical confinement layer in output efficiency deterioration of laser diodes," in *Proceedings of the 25th IEEE International Semiconductor Laser Conference*, Kobe, Japan, 12–15 Sep 2016 (IEEE, 2016).
[18]L. A. Coldren and S. W. Corzine, *Diode Lasers and Photonic Integrated Circuits* (Wiley, New York, 1995).
[19]S. Rauch, H. Wenzel, M. Radziunas, M. Haas, G. Trankle, and H. Zimer, Appl. Phys. Lett. **110**, 263504 (2017).
[20]E. A. Avrutin and B. S. Ryvkin, Semicond. Sci. Technol. **32**, 015004 (2017).
[21]M. R. Gokhale, J. C. Dries, P. V. Studenkov, S. R. Forrest, and D. Z. Garbuzov, IEEE J. Quantum Electron. **33**, 2266 (1997).